A REFINED OPTICAL TECHNIQUE FOR THE MEASUREMENT OF ULTRASONIC ABSORPTION

Thesis for the Degree of M. S.

MICHIGAN STATE UNIVERSITY
WILLIAM J. TACZAK

1968

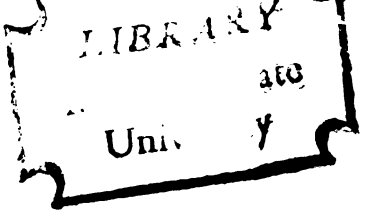

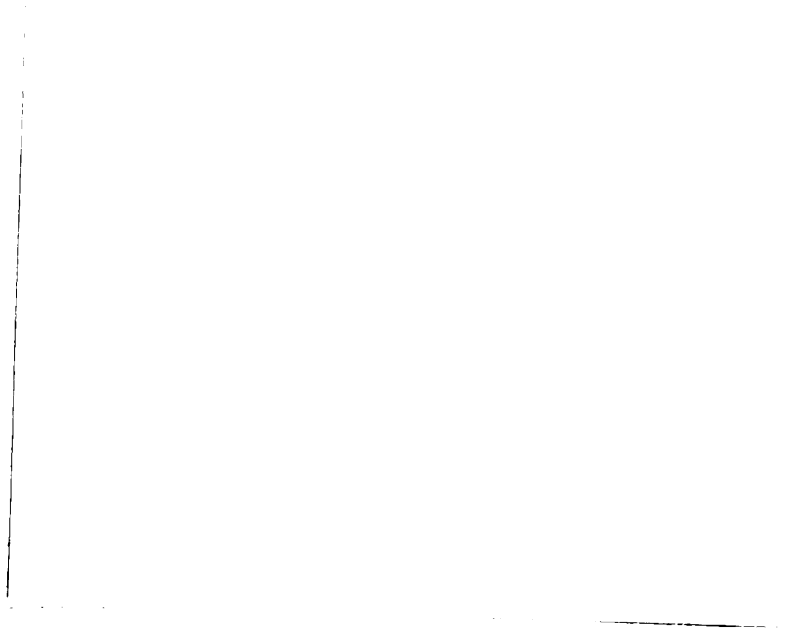

ABSTRACT

A REFINED OPTICAL TECHNIQUE FOR THE MEASUREMENT OF ULTRASONIC ABSORPTION

by William J. Taczak

The optical method has been used quite extensively for the measurement of ultrasonic absorption in liquids. However, acoustic diffraction has limited the accuracy of such measurements because of large local variations in the optical effect. It is shown in this paper, both theoretically and experimentally, that a light beam traversing an acoustic beam radiated from a square transducer, parallel to a diagonal of the transducer, produces an on-axis integrated optical effect that is nearly constant in the near field of the sound beam. In the present experiment, absolute and relative ultrasonic absorption coefficients are determined for aqueous solutions of the electrolytic salt, manganese sulfate. Absolute ultrasonic absorption measurements are made in this region by assuming that the on-axis effect is constant. For relative ultrasonic absorption measurements, the following procedure is used: (1) the integrated optical effect is measured in water, which has negligible acoustic absorption; (2) the total optical effect is measured with manganese sulfate added to the water; and (3), (1) is divided into (2) to correct for the acoustic diffraction. With proper experimental care and with a nearly constant region of sufficient range, relative measurements will give reliable values for ultrasonic absorption coefficients to $\alpha = .001\ cm^{-1}$.

A REFINED OPTICAL TECHNIQUE FOR THE MEASUREMENT OF ULTRASONIC ABSORPTION

by

William J. Taczak

A THESIS

Submitted to
Michigan State University
in partial fulfillment of the requirements
for the degree of

MASTER OF SCIENCE

Department of Physics

1968

ACKNOWLEDGMENT

The author wishes to express his gratitude to Professor E. A. Hiedemann and Dr. B. D. Cook for their guidance in this work. The discussions with Dr. F. Ingenito also have been very helpful. The financial support of this research by the Office of Naval Research is gratefully acknowledged.

TABLE OF CONTENTS

LIST OF FIGURES

CHAPTER I

INTRODUCTION

Optical methods have been used by many investigators for the measurement of ultrasonic absorption in liquids. The methods have been restricted to ultrasonic frequencies above 2 mHz., because, at low frequencies, the ultrasonic absorption is very small, requiring the measurement to be made over a substantial path length in order to obtain measurable effects. However, over large path lengths, diffraction of the acoustic beam becomes significant. In addition, the angular separation of the optical diffraction orders is proportional to the ultrasonic frequency, and at low frequencies, it becomes difficult, if not impossible, to isolate an individual diffraction order.

The latter difficulty can be overcome by keeping the optical configuration constant. The more serious problem, diffraction of the acoustic beam, is illustrated in Figure 1a[1], a schlieren photograph of the sound field radiated by a square transducer, with the light beam traversing the sound field parallel to one of the transducer sides. The darker areas in the photograph correspond to regions of higher acoustic pressure. It can be seen that the diffraction of the acoustic beam produces large variations of the optical effect over relatively small regions. In making an absorption measurement, the sound field is sampled by a narrow light beam and the optical effects at various distances from the source

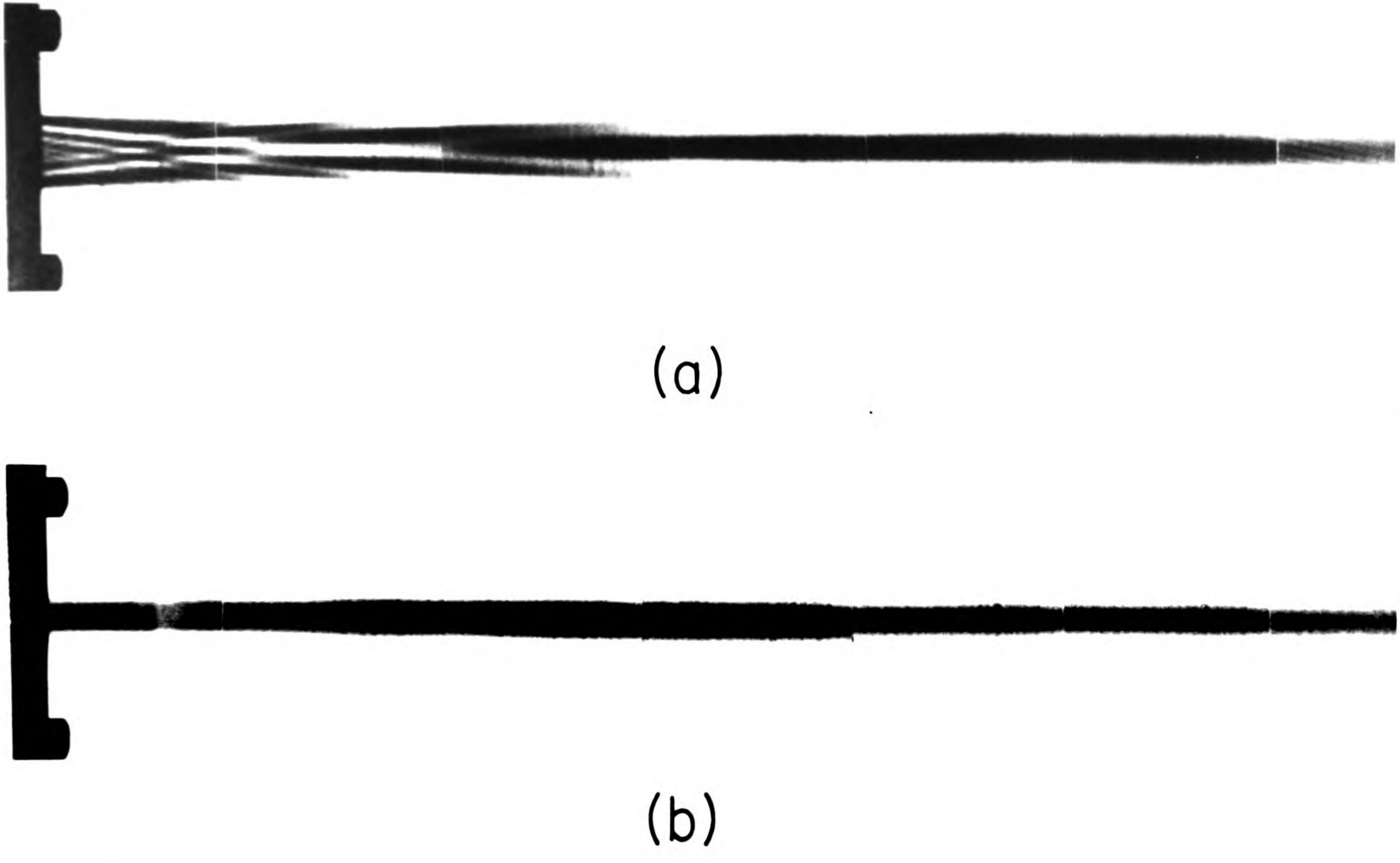

Figure 1. Schlieren photograph of the sound field produced by a square transducer with the light beam crossing the sound field parallel to (a) one of the sides of the transducer, and (b) a diagonal of the transducer.

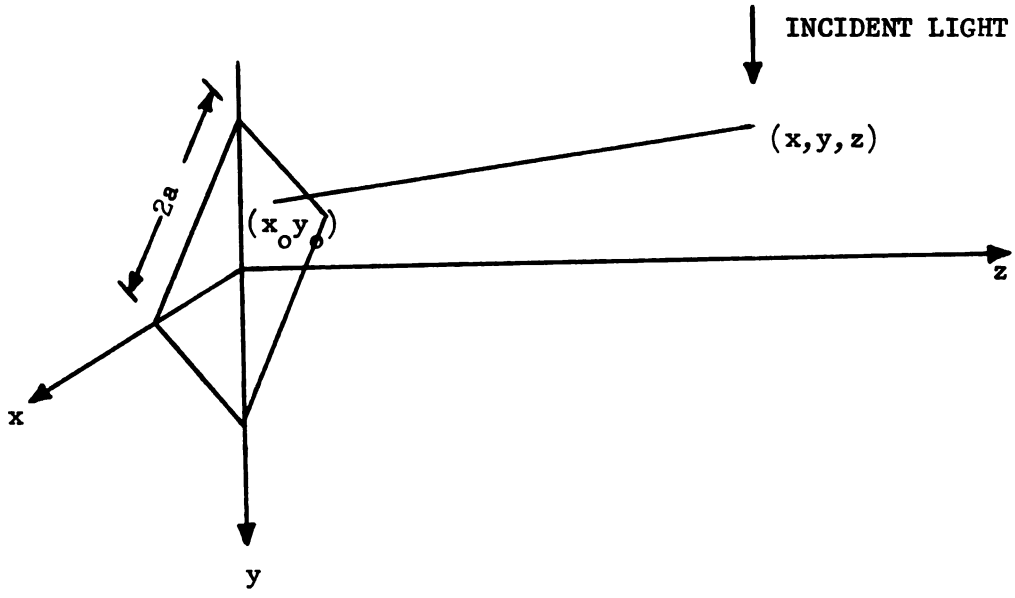

Figure 2. Coordinate System of Transducer Configuration

are compared. It is clear that the large variations due to the diffraction of the acoustic beam will tend to obscure the effect of absorption.

Recently, Cook and Ingenito[1] have devised a transducer configuration which produces a slowly varying optical effect in the near field of the transducer. Figure 1b[1] is a photograph of the schlieren pattern produced by a square transducer with the light beam traversing the sound field parallel to a diagonal of the square. In this case, the optical effect is nearly uniform close to the axis of the sound beam. Cook and Ingenito have also calculated the theoretical on-axis expressions corresponding to Figures 1a and 1b, and their results agree with the experiment.

In the next section, we derive an expression for the on-axis optical effect of the transducer configuration shown in Figure 2,

and it is shown that the resulting expression is the product of the non-absorptive result of Cook and Ingenito and an exponential absorption factor. In a later section we describe the measurement of the ultrasonic absorption in aqueous solutions of manganese sulfate using the transducer configuration of Figure 2. Our technique consists of measuring the total optical effect and dividing out the non-absorption result, which is due to the transducer configuration, leaving the factor that is due to the absorption of the solution, from which the absorption coefficient can be found. Aqueous solutions of the electrolytic salt $MnSO_4$ were chosen because (1) manganese sulfate has a convenient relaxation frequency of about 3 mHz., (2) reasonable solution concentrations produce measurable absorption and (3) other experiments have been done with this salt and these will be used for comparison.

CHAPTER II

THEORY

In the presence of a sound beam, the local optical refractive index is altered through the changes in density of the liquid induced by the sound waves. If the sound beam ideally consists of plane waves localized in a beam of width L, the region containing the sound beam would act as a thick optical phase grating. The nature of the diffraction of the light depends not only upon the change of refractive index and the width of the sound field, but also upon certain combinations of the wavelengths, λ and λ^*, of the light and sound respectively, with the width L and the angle of incidence of the light beam[2]. At low frequencies and for the light beam at normal incidence to the sound beam, many of the multiple interference effects vanish and the diffraction phenomena can be described by assuming that the sound beam acts as a simple phase grating. That is, for a plane light wave impinging of the sound beam, only the phase of the light beam is modified and there is no amplitude modulation. For light traveling in the y direction and the sound in the z direction, the modulation of the light can be described as

$$E = E_o \, e^{i(ky-\omega t)} \, e^{iV(x,z,t)} \quad , \tag{1}$$

where

$$V(x,z,t) = \frac{2\pi K}{\lambda} \int_{-\infty}^{+\infty} p(x,y,z,t) \, dy \quad . \tag{2}$$

In Eq. 2, κ is the piezooptic coefficient of the liquid and $p(x,y,z,t)$ is the localized acoustic pressure in the liquid. For the idealized situation of plane sound waves of acoustic pressure $p = p_o \sin (k^* z - \omega^* t)$, the light is diffracted into discrete diffraction orders with the angular separation

$$\sin \theta_n = \frac{n\lambda}{\lambda^*} \quad , \tag{3}$$

and normalized intensity

$$I_n = J_n^2(v) \quad , \tag{4}$$

where J_n is the ordinary Bessel function and $v = \frac{2\pi\kappa}{\lambda} p_o$.

In the practical situation, these results are modified by diffraction of both the light and the sound, as beams of finite width are necessary. Limiting the size of the optical beam so it is comparable to the acoustic wavelength causes an angular spreading of the diffraction orders, even to the point of overlapping. The acoustical beam radiating from a transducer of finite size is not confined to a collimated beam, but undergoes Fresnel diffraction in the region near the transducer. This diffraction causes $p(x,y,z,t)$ to vary locally in space, both in magnitude and phase. Integration over y of $p(x,y,z,t)$ in Eq. 2 yields a $V(x,z,t)$, the magnitude of which varies with both x and z because of diffraction.

It is desirable to have the variations of $V(x,z,t)$, arising from the acoustical diffraction, to be as small as possible when using the optical technique for absorption measurements. As

the diagonal transducer configuration, discussed earlier, provides a means of reducing the variations, we shall theoretically calculate the integrated optical parameter $V(x,z,t)$ from a sound field produced by this configuration. Since the schlieren photograph in Figure 1b indicates that the integrated optical effect does not vary much in a region near the transducer axis, only the axial values will be calculated.

In order to obtain the integrated optical effect, an expression for the sound pressure field of a square transducer must first be found. Then the optical effect of a light beam traveling through the sound field, parallel to a diagonal of the transducer can be determined.

Consider a square transducer of side 2a, in an infinite rigid mounting, radiating into a fluid of average density ρ_o. The transducer is assumed to act as a plane piston, so that every point on its face has a velocity $u = u_o e^{-i\omega^* t}$ normal to the piston face, where u_o is a constant and ω^* is the angular frequency. The transducer is parallel to the x-y plane and a diagonal lies on the y-axis. See Figure 2.

To find the acoustic pressure at some point (x,y,z), the contribution from an infinitesimal element of the transducer is first considered. According to Huygens' principle, the infinitesimal element dS (point source) will radiate a hemispherically symmetric wave producing, at a distance R, a pressure dp of the form

$$dp = \frac{-i\rho_o u_o \omega^*}{2\pi} \frac{e^{i(K^* R - \omega^* t)}}{R} dS \quad , \tag{5}$$

where $K^* = K_r + i\alpha$ and $\alpha > 0$. The complex propagation constant K^* includes the absorption coefficient α of the medium, in addition to the real propagation constant K_r. If we integrate over the surface S of the transducer, the acoustical pressure at (x,y,z) will be

$$p(x,y,z) = \frac{-i\rho_o u_o \omega^*}{2\pi} \int_S \frac{e^{iK^* R}}{R} dx_o \, dy_o \quad , \tag{6}$$

where the time dependence $e^{-i\omega^* t}$ is understood and

$$R = [(x-x_o)^2 + (y-y_o)^2 + z^2]^{1/2} \tag{7}$$

is the distance between a point on the transducer face $(x_o, y_o, 0)$ and a field point (x,y,z). Having found the sound pressure, we can now calculate the integrated optical effect.

By substituting Eq. 6 into Eq. 2, we can write the integrated optical effect as

$$V(x,z) = \frac{-i\rho_o u_o \omega^* \kappa}{\lambda} \int_{-\infty}^{\infty} dy \int_S dx_o dy_o \frac{e^{iK^*[(x-x_o)^2+(y-y_o)^2+ z^2]^{1/2}}}{[(x-x_o)^2 + (y-y_o)^2 + z^2]^{1/2}} . \tag{8}$$

By changing the order of integration, and using the following relation[3],

$$\int_{-\infty}^{\infty} \frac{e^{iK^*[(x-x_o)^2+(y-y_o)^2+ z^2]^{1/2}}}{[(x-x_o)^2+(y-y_o)^2+ z^2]^{1/2}} dy = i\pi H_o^{(1)} \left\{ K^*[(x-x_o)^2+ z^2]^{1/2} \right\} , \tag{9}$$

the expression for Eq. 8 becomes

$$V(x,z) = \frac{\pi\rho_o u_o \omega^* \kappa}{\lambda} \int_S dx_o dy_o \, H_o^{(1)}\left\{K^*[(x-x_o)^2 + z^2]^{1/2}\right\} . \qquad (10)$$

Since we are interested in obtaining the on-axis effect, one can see that with x = 0, the symmetry of Eq. 10 is such that its result is equivalent to four times the result of one quadrant of the transducer. Using this fact, and setting x = 0, Eq. 10 becomes

$$V(0,z) = \frac{4\pi\rho_o u_o \omega^* \kappa}{\lambda} \int_0^{\sqrt{2}a} dx_o \int_0^{\sqrt{2}a-x_o} dy_o \, H_o^{(1)}\left\{K^*[x_o^2 + z^2]^{1/2}\right\} . \qquad (11)$$

The Hankel function $H_o^{(1)}$ is not a function of y_o, and we are left with a single integral. Using the standard result that

$$\int \beta \, H_o^{(1)}(a\beta) \, d\beta = \frac{\beta}{a} H_1^{(1)}(a\beta) , \qquad (12)$$

the on-axis integrated optical effect becomes

$$V(0,z) = \frac{4\pi\rho_o u_o \omega^* \kappa}{\lambda} \left\{\sqrt{2}\, a \int_0^a H_o^{(1)}\left\{K^*[x_o^2 + z^2]^{1/2}\right\} dx_o \right.$$

$$\left. - \frac{[z^2 + 2a^2]^{1/2}}{K^*} H_1^{(1)}\left\{K^*[z^2 + 2a^2]^{1/2}\right\} + \frac{z}{K^*} H_1^{(1)}[K^* z]\right\} . \qquad (13)$$

The expression can be further simplified if we consider the case where $\sqrt{2}\, K^* a \gg 1$ and $z^2 \gg a^2$. For large values of the argument θ, the Hankel functions can be approximated as[4]

$$H_o^{(1)}(\theta) \approx \left(\frac{2}{\pi\theta}\right)^{1/2} e^{i(\theta - \pi/4)} , \tag{14}$$

and

$$H_1^{(1)}(\theta) \approx \left(\frac{2}{\pi\theta}\right)^{1/2} e^{i(\theta-3\pi/4)} . \tag{15}$$

Using these expressions in Eq. 9, we get

$$V(0,z) = \frac{4\pi\rho_o u_o \omega^* \kappa}{\lambda}\left\{\left(\frac{4a^2}{\pi K^*}\right)^{1/2} \int_0^{\sqrt{2}\,a} \frac{e^{i[K^*(x_o^2+ z^2)^{1/2} - \pi/4]}}{(x_o^2+ z^2)^{1/4}}\, dx_o \right.$$

$$- \frac{(z^2+ 2a^2)^{1/2}}{K^*}\left[\frac{2}{\pi K^*(z^2+ 2a^2)^{1/2}}\right]^{1/2} e^{i[K^*(z^2+ 2a^2)^{1/2} - 3\pi/4]} \tag{16}$$

$$\left. + \frac{z}{K^*}\left(\frac{2}{\pi K^* z}\right)^{1/2} e^{i(K^* z - 3\pi/4)}\right\} .$$

In Eq. 16, the exponential factors in the numerators vary more rapidly with z than the demoninators; hence, more care must be given to approximating the exponentials. Expanding the exponents by the binomial series, and neglecting all terms in the denominator except z, we get from Eq. 16,

$$V(0,z) = 2\rho_o u_o \omega^* \kappa\, e^{i(K^* z - \pi/4)}\left\{\left(\frac{4a^2 K^*}{\pi z}\right)^{1/2} \int_0^{\sqrt{2}\,a} e^{iK^* x_o^2/2z}\, dx_o \right.$$

$$\left. + i\left(\frac{2z}{\pi K^*}\right)^{1/2} (e^{iK^* a^2/z} - 1)\right\} . \tag{17}$$

Finally, the on-axis integrated optical effect can be expressed as

$$V(0,z) = 2\rho_o u_o \omega^* \kappa \, e^{i(K_r z - \pi/4)} \left\{ C(\delta) + iS(\delta) + i(\pi\delta)^{-1}\left(e^{\frac{i\pi\delta^2}{2}} - 1\right)\right\} e^{-\alpha z}, \quad (18)$$

where $\delta^2 = \frac{2K^* a^2}{\pi z}$,

and $$C(\delta) = \int_o^\delta \cos \frac{\pi}{2} t^2 \, dt \quad , \quad (19)$$

$$S(\delta) = \int_o^\delta \sin \frac{\pi}{2} t^2 \, dt \quad , \quad (20)$$

are Fresnel integrals.

For liquids with low absorption coefficients, $|K_r| \gg |\alpha|$, so that we can write $\delta^2 \approx \frac{2K_r a^2}{\pi z}$. Equation 18 is now the product of a factor that is due to the transducer configuration, and an exponential, $e^{-\alpha z}$, that is due to the absorption of the medium. By plotting $V(0,z)$ as a function of δ, excluding the absorption term, one can see in Fig. 3, a flat region for $1.45 < \delta < 2.20$ where the effect remains nearly constant.

At this point, the question arises as to how well the theoretical curve agrees with experimental results - if the theory correctly predicts the position, range and "flatness" of the integrated optical effect in the near field for the chosen transducer configuration. We also are confronted with the problem of whether the nearly constant

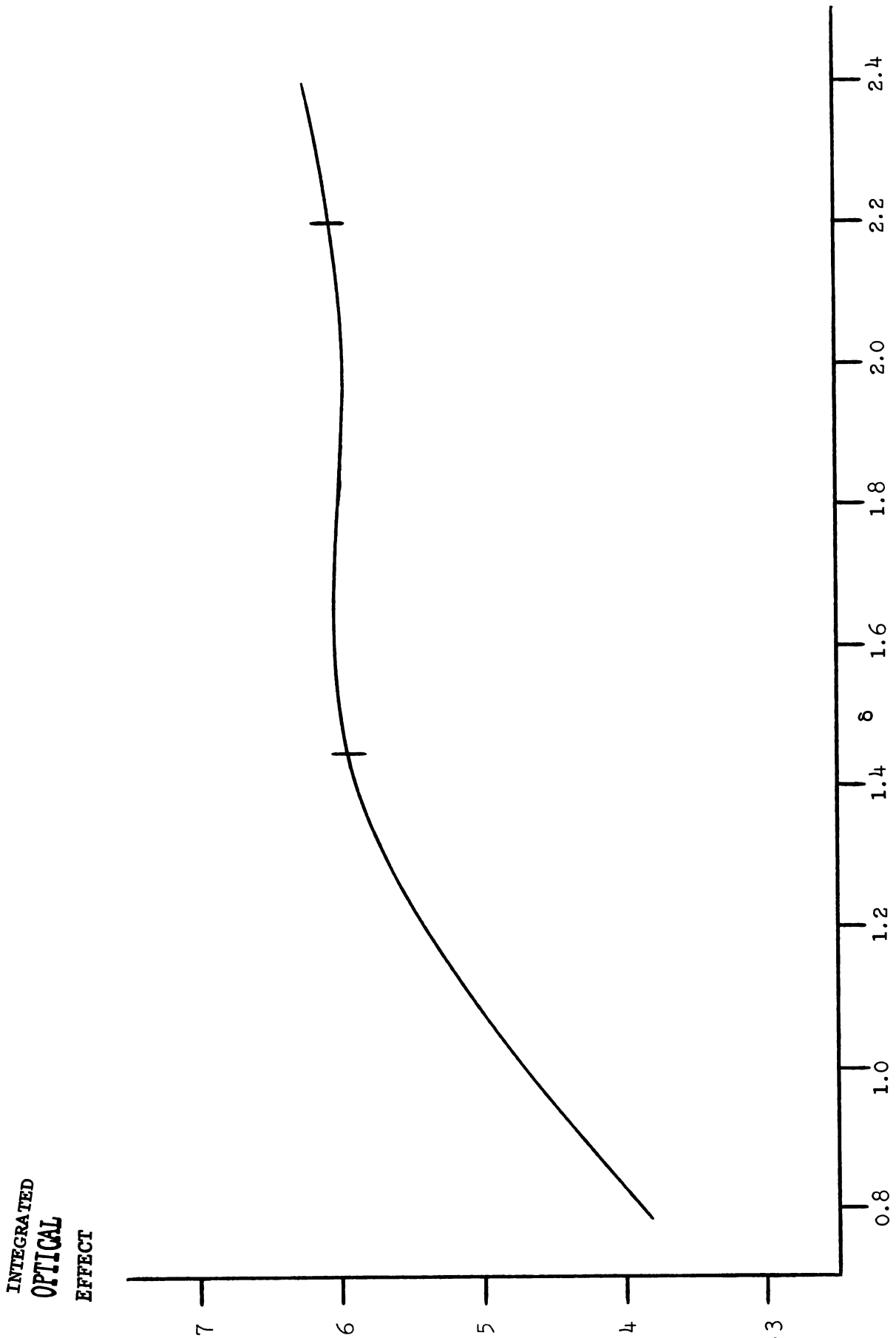

Figure 3. Theoretical curve of the integrated optical effect for a light beam crossing the sound field, radiated by a square transducer, parallel to one of the transducer diagonals.

integrated optical effect can be useful in obtaining meaningful and reproducible ultrasonic absorption measurements, and, if so, what the limits are for reliable results. These questions form the basis for the present experiment and will be explored in later sections.

CHAPTER III

EXPERIMENTAL STUDY

A schematic diagram of the Debye-Sears optical method used for the absorption measurements is shown in Fig. 4.

The transducer assembly consists of a holder that provides air backing for a circular, x-cut quartz transducer. A square electrode painted in the center of the transducer with metallic silver paint gave the desired transducer configuration. The transducer assembly is mounted on an overhead optical rail and can vary 0.5 to 30.0 cm. from the light beam. Transducers of different thickness can be easily interchanged in the holder. The resonant frequency of each transducer is obtained by adjusting the radio frequency transmitter to a frequency that produces the maximum number of optical diffraction orders for a fixed r.f. voltage. The transducers vary in resonant frequencies from 300 kHz. to 7.5 mHz.

The sound beam is adjusted to be normal to the light beam by means of two screws on the transducer holder, which pivot the transducer about two perpendicular axes in the plane of the transducer face. The sound and the light are judged to be normal when the maximum light diffraction occurs and the zero order light intensity is a minimum, for small acoustic intensities[5].

In order to orient the square transducer so that a diagonal is parallel to the direction of propagation of the light beam, the transducer holder is rotated about an axis perpendicular to the center of the transducer face, while observing the schlieren pattern

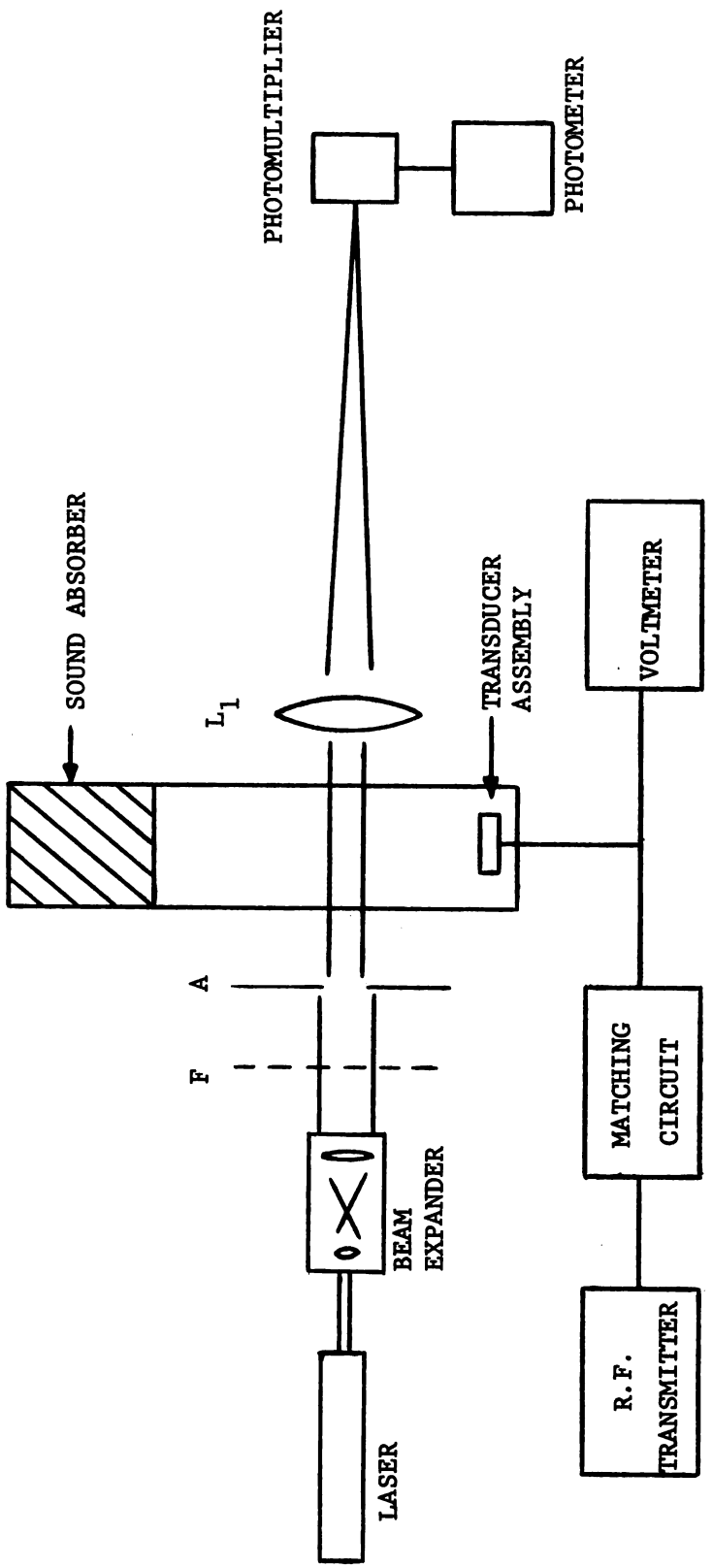

Figure 4. Schematic diagram of experimental arrangement.

of the sound beam. It is found that changes in the integrated optical effect are symmetric about the desired position.

The optical system consists of the following: a He-Ne gas laser; a beam expander that spatially filters and recollimates the light; lens L_1, which focuses the optical diffraction pattern on a plane at the entrance slit of the photomultiplier; and a photometer, which records the relative intensity of light entering the photomultiplier. The filter is inserted to reduce the intensity of the laser beam so that the entrance slit of the photomultiplier can be opened to a suitable width. If the entrance slit is too narrow, instabilities occur due to mechanical vibrations of the optical system. An aperture A of 2 mm. diameter allows the light beam to pass only through the center of the symmetrical sound field.

The photomultiplier is set on the zeroth order of the optical diffraction pattern to measure the light intensity as a function of r.f. potential. The zeroth order was chosen for the following reason. An ultrasonic wave of finite amplitude that is initially sinusoidal becomes saw-toothed-shaped as it propagates away from the source. The saw-toothed waves produce an asymmetrical optical diffraction pattern. Nomoto and Kegishi[6] have theoretically shown that while the higher orders of the optical diffraction pattern are greatly affected by finite amplitude waves, the zeroth order is not. In fact, the intensity of the zeroth order is the same whether sinusoidal or saw-toothed waves exist when the Raman and Nath phase

grating approximation is applicable.

From Raman and Nath theory, the intensity of the zeroth order of the diffraction pattern is given by Eq. 4. The relative acoustical effect is determined from 1/E, where E is the r.f. potential needed for a constant I_o. The largest gradient in I_o for an incremental change in v can be shown to be $I_o \approx 50\%$ of its maximum value. Thus, the greatest accuracy for determining the applied potential can be attained for this constant value of I_o. The quantity 1/E is proportional to V and includes the effects of both the transducer configuration and the acoustic absorption of the fluid.

For frequencies less than 1 mHz., the distance between the optical diffraction orders is so small that the orders overlap. The intensity recorded by the photomultiplier is still primarily due to the zeroth order, but now a small function of the light intensity is due to higher orders. Fortunately, the finite amplitude effects of the higher orders are quite small at low frequencies and do not affect the accuracy of the absorption measurements. The problem of overlapping orders is solved by keeping the optical configuration constant during the experiment.

CHAPTER IV

RESULTS

The first problem to be considered is to determine how well the theoretical curve predicts the measured on-axis integrated optical effect. Water is used to investigate the on-axis effect, since the acoustic absorption is not significant over the desired range of measurements. In Fig. 5, the experimental results are compared to the theoretical curve, calculated from Eq. 18. As one can see, the two curves are not perfect fits, with differences up to 3% in the predicted flat region. This is interpreted to mean that the theoretical on-axis integrated optical effect can be used when the exponential decay due to the ultrasonic absorption is much greater than the error between the two curves. For practical purposes, the on-axis effect is assumed to be constant and an absolute absorption measurement is made. When the ultrasonic absorption is quite small, the error of 3% becomes significant, and an absolute absorption coefficient cannot be determined. For the latter condition, the on-axis effect must be determined experimentally for each individual case, and a relative change in absorption can be measured, for example, when small amounts of electrolytic salts are added to water.

Aqueous solutions of the polyvalent electrolytic salt, manganese sulfate, were chosen for the present experiment, for reasons stated earlier. Measurements were taken for frequencies in the range 0.3 to 7.5 mHz. at solution concentrations of 0.01 to 0.5 m. Kurtz and Tamm[7], Smithson and Litovitz[8] and Kor and Verma[9]

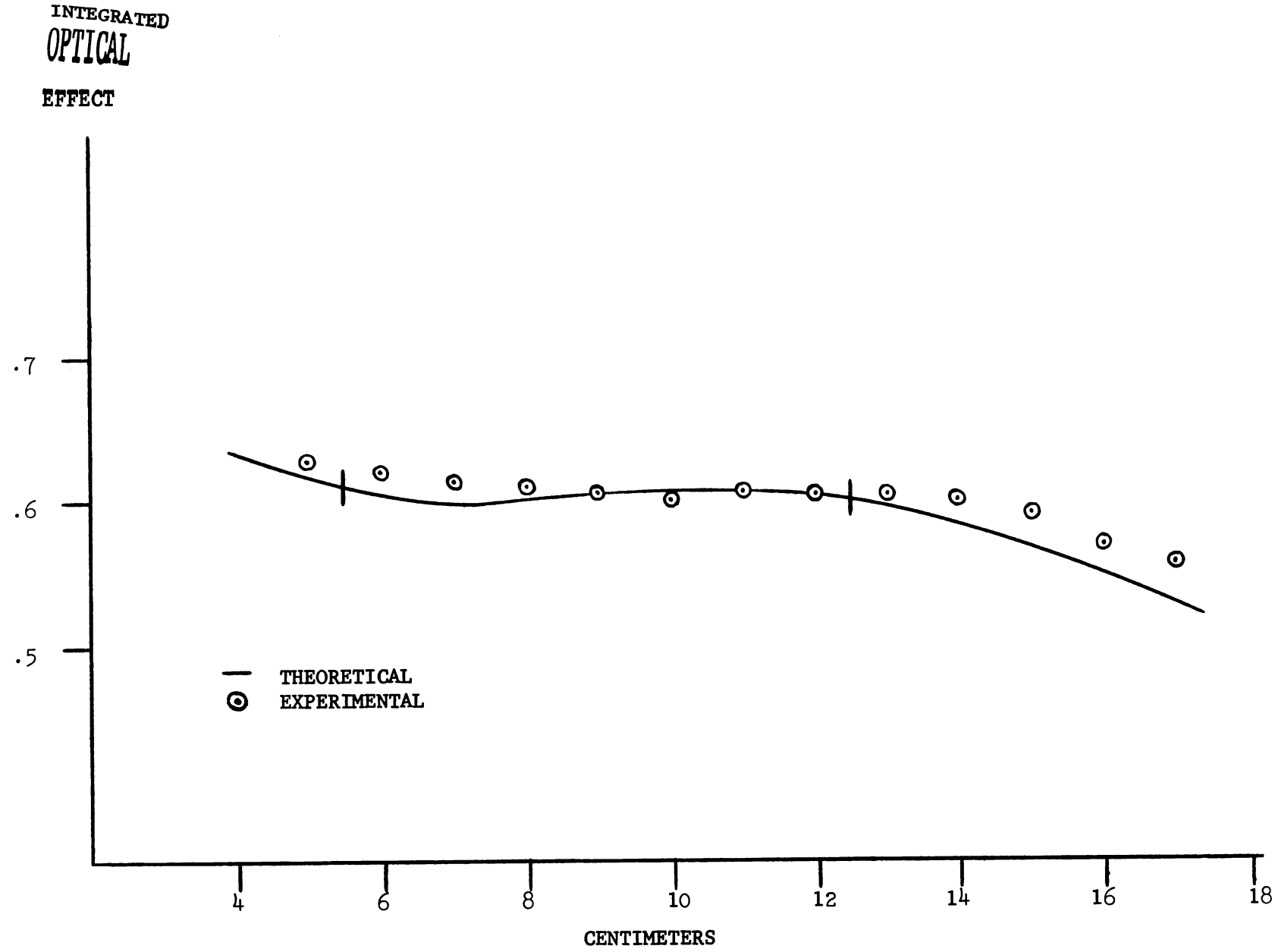

Figure 5. Comparison of theoretical and experimental results; normalized to flat region ($f^* = 4.0$ mHz., $a = 0.5$ cm.)

performed similar experiments with $MnSO_4$ in the frequency range of present interest, using various techniques, as shown in Fig. 6.

Absolute absorption measurements were taken over the range of frequencies for a fixed solution concentration of 0.1 m and constant temperature of 21.5°C. Figure 7 shows the dependence of α/f^{*2} on frequency. The curve has a constant value at low frequencies and decreases with increasing frequency. For frequencies greater than 1 mHz, our results are somewhat lower than those of Kurtz et.al. and Kor et. al. With increasing frequency, the curves begin to approach each other due to the increasing importance of the absorption of water. For frequencies less than 1 mHz., we found that the parameter α/f^{*2} begins to level off at about 1.5×10^{-14} $sec^2/cm.$, more than double the results of Kor et. al. The only explanation given for the different results is that the error associated with the determination of absolute absorption coefficients by the optical technique is large at low frequencies. The relaxational nature of $MnSO_4$ is illustrated in Fig. 8, which is a plot of the parameter

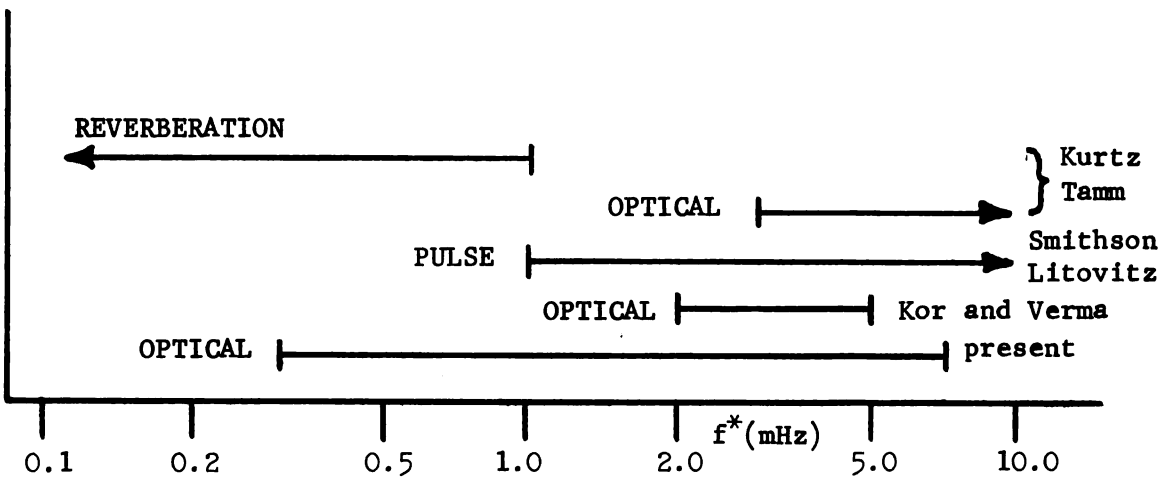

Figure 6. Frequency Range of Various Techniques Used for Measuring the Ultrasonic Absorption in $MnSO_4$.

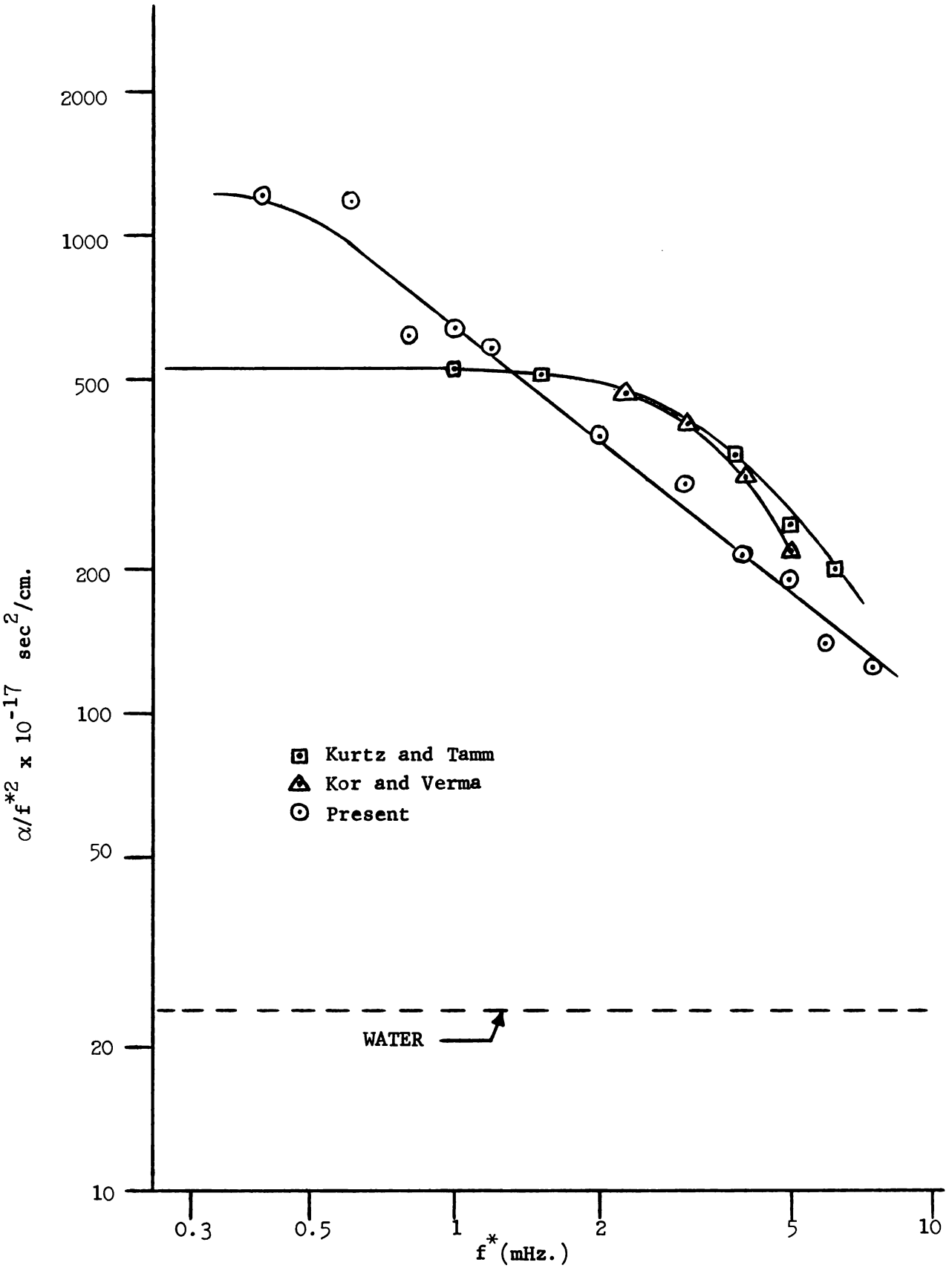

Figure 7. Parameter α/f^{*2} vs. acoustical frequency for 0.1 M $MnSO_4$ at 21.5°C.

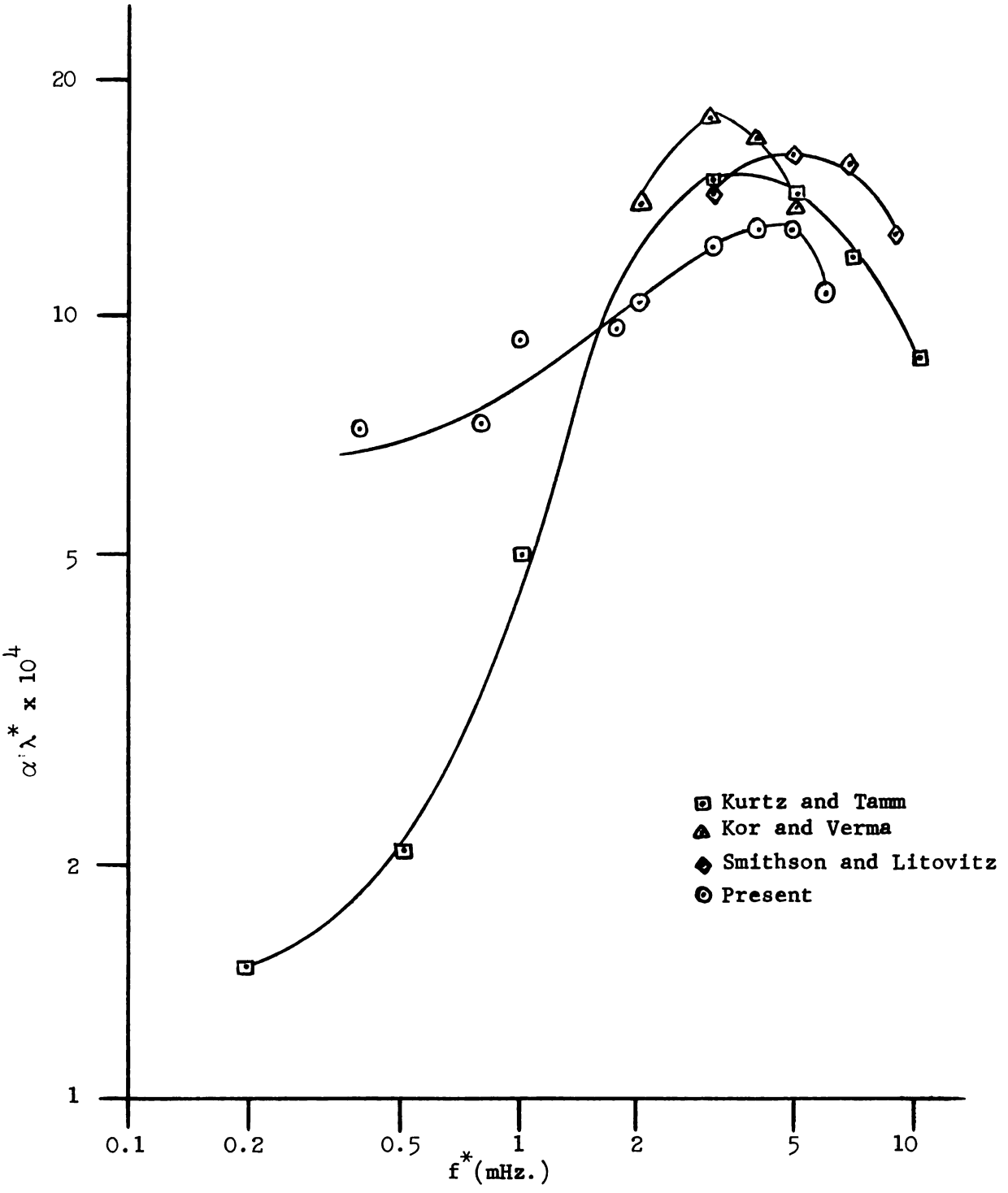

Figure 8. Parameter $\alpha'\lambda^*$ vs. acoustical frequency for 0.1 m $MnSO_4$ at 21.5°C.

$\alpha'\lambda^*$ vs. frequency. α' is the excess absorption due to the salt, defined as $\alpha' = \alpha_{solution} - \alpha_{water}$. Our results show a relaxation peak near 4 mHz. with somewhat smaller value than the results of others, and does not drop off as rapidly at lower frequencies as the curve of Kurtz et. al.

Figure 9 shows the effect of various concentrations of $MnSO_4$ on the relative measurements of ultrasonic absorption at the fixed frequencies of 0.8 and 4.0 mHz. At 4.0 mHz., the absorption increases very linearly for concentrations from 0.01 to 0.3 m, and increases slightly less than linearly for higher concentrations. There is little agreement between our results and the non-linear results of Kor et. al. at 4.0 mHz. The ultrasonic absorption at 0.8 mHz also appears to increase linearly for concentrations from 0.05 to 0.5 m.

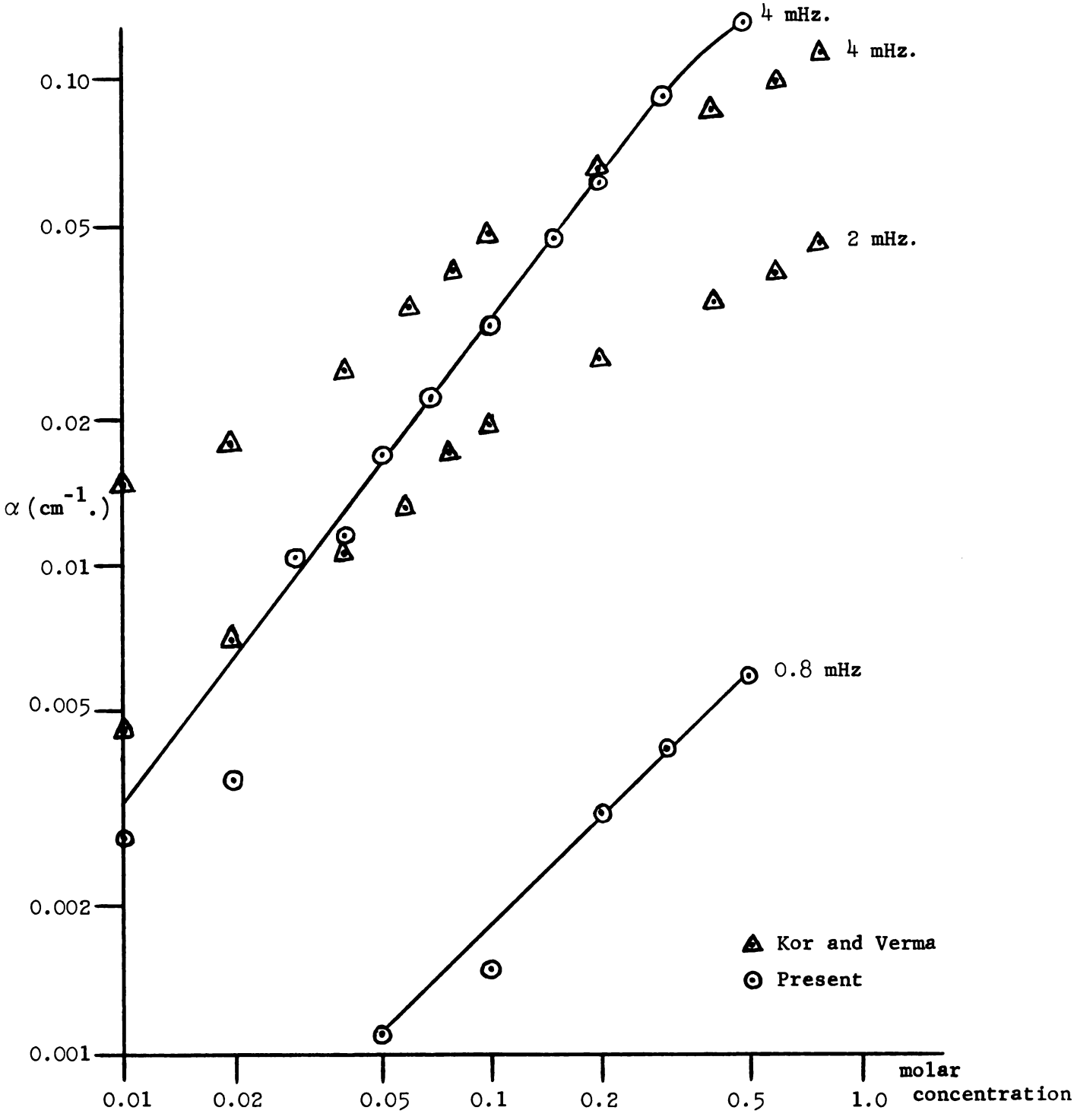

Figure 9. Relative absorption coefficient α vs. solution concentration of $MnSO_4$.

CHAPTER V

CONCLUSION

It has been shown, both theoretically and experimentally, that a light beam traversing an acoustic beam radiated by a square transducer, parallel to a diagonal of the transducer, produces an integrated optical effect that is nearly constant in the Fresnel field of the sound beam. Figure 5 shows that the calculated and experimental results, when normalized to the flat region, agree quite well in the near field, but differ as to where the optical effect begins to fall off. The theory is quite satisfactory for our purpose, as we are concerned only with the flat region of the integrated optical effect. Using the flat region for absorption measurements has produced results comparable to those of other investigators, though our results are generally lower. The optical method for absorption measurements is not limited to plane acoustic waves, as earlier, since the optical effect can now be determined by integrating across the sound beam. With proper experimental care and with a nearly constant optical effect of sufficient range, relative measurements will give reliable values for ultrasonic absorption coefficients to $\alpha = .001\ cm^{-1}$.

BIBLIOGRAPHY

1. B. Cook and F. Ingenito, to be published in Proc. IEEE.

2. W. Klein and B. Cook, IEEE Trans. on Sonics and Ultrasonics, 14, 126 (1967).

3. W. Magnus and F. Oberhettinger, Functions of Mathematical Physics, Chelsa Publishing Co. (1949), p. 27.

4. See Reference 3, p. 22.

5. C. Raman and N. Nath, Proc. Indian Acad. Sci. A2, 413 (1935).

6. O. Nomoto and K. Negishi, Acustica 15, 223 (1965).

7. G. Kurtz and K. Tamm, Acustica 3, 33 (1953).

8. J. Smithson and T. Litovitz, J. Acoust. Soc. Am. 28, 462 (1956).

9. S. Kor and G. Verma, J. Chem. Physics 29, 9 (1958).